Supporting Information

Mononuclear Lanthanide Complexes Assembled from a Tridentate NNO Donor Ligand: Design of a Dy^{III} Single-Ion Magnet

Pankaj Kalita,[a] Amit Malakar,[a,d] Joydeb Goura,[a,c] Subhashree Nayak,[a] J. M. Herrera[b] Enrique Colacio[b] and Vadapalli Chandrasekhar*[c,d]*

[a]School of Chemical Sciences, National Institute of Science Education and Research Bhubaneswar, HBNI, Jatni, Khurda - 752050, Odisha, India

[b]Departamento de Química Inorgánica, Facultad de Ciencias, Universidad de Granada, Avenida de Fuentenueva s/n, 18071 Granada, Spain

[c]Department of Chemistry, Indian Institute of Technology Kanpur, Kanpur-208016, India

[d]Tata Institute of Fundamental Research Hyderabad, Gopanpally, Hyderabad-500107, India

AUTHOR EMAIL ADDRESSES: vc@iitk.ac.in; vc@tifrh.res.in

ecolacio@ugr.es

Contents

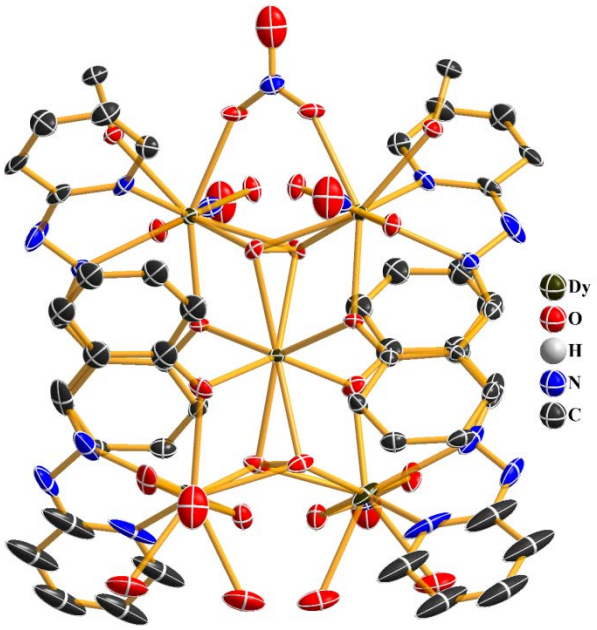

Figure S1. Molecular structure of complex $[Dy_5(L)_4(NO_3)_5(HOMe)_2(O_2)_2(H_2O)_4]^{2+}$ with thermal ellipsoids of 30 % probability level (H-atoms and counter NO_3^- anions are omitted for clarity)

Table 1. Crystal data and structure refinement for Dy_5 complex

Empirical formula	C50H60Dy5N19O37
Formula weight	2331.67
Temperature/K	120.00(10)
Crystal system	Trigonal
Space group	*P*3121
a/Å	14.6240(4)
b/Å	14.6240(4)
c/Å	31.1799(11)
α/°	90
β/°	90
γ/°	120
Volume/Å^3	5774.8(4)
Z	3
ρ_{calc}g/cm^3	2.011

μ/mm^{-1}	4.893
F(000)	3357.0
Crystal size/mm^3	0.18 × 0.15 × 0.11
Radiation	MoKα (λ = 0.71073)
2Θ range for data collection/°	5.572 to 58.25
Index ranges	$-19 \leq h \leq 15$, $-16 \leq k \leq 19$, $-41 \leq l \leq 42$
Reflections collected	52102
Independent reflections	9359 [R_{int} = 0.0986, R_{sigma} = 0.0810]
Data/restraints/parameters	9359/46/404
Goodness-of-fit on F^2	1.024
Final R indexes [I>=2σ (I)]	R_1 = 0.0535, wR_2 = 0.1366
Final R indexes [all data]	R_1 = 0.0744, wR_2 = 0.1455
Largest diff. peak/hole / e $Å^{-3}$	2.32/-2.18
Flack parameter	0.010(12)
CCDC Number	1891540

Synthesis of Ligand HL

A methanolic solution of 2-hydrazino pyridine (600 mg, 5.45 mmol) was taken in a 100 ml round bottom flask and stirred for ten minutes. To it a methanolic solution of 2-hydroxy-5-nitro benzaldehyde (900 mg, 5.38 mmol) was added. The solution was then heated to reflux for 6 hours. During this time a yellow colored precipitate was obtained. After cooling, the precipitate was filtered out and washed with cold methanol followed by diethyl ether. The precipitate was finally dried under vacuum and the product was obtained in 92% yield (1.3 g). The melting point and other experimental characterization data are as follows: M.P.: 240 $^{\circ}$C. IR (KBr ν/cm^{-1}): 1606(s), 1520(m), 1482(m), 1442(s), 1348(s), 1303(s), 1170(m), 1096(m), 994(w), 924(m), 828(m), 772(m), 718(w), 638(w). ^{1}H NMR ([D6]DMSO, δ, ppm): 11.09 (s, 1H, N-H), 8.49 (d,

1H, Ar-H), 8.25 (s, 1 H, imine H), 8.09 (dd, 1H, Ar-H), 7.66-7.60 (m, 1H, Ar-H), 7.10 (d, 1H, Ar-H), 7.00 (d, 1H, Ar-H), 6.77-6.73 (m, 1H, Ar-H). ESI-MS (m/z) ($M + H^+$) = 259.0881.

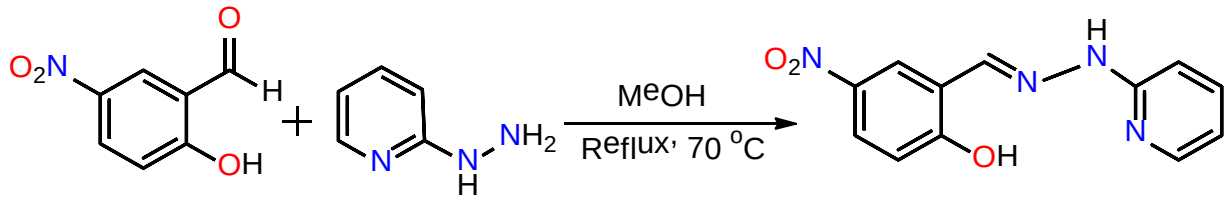

Scheme S1. Synthesis of the ligand HL.

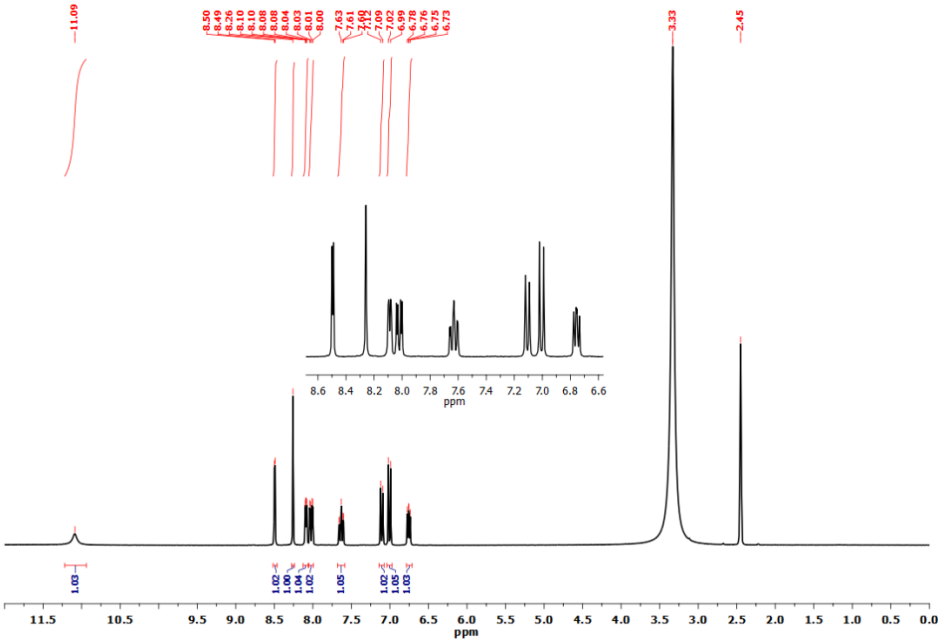

Figure S2. ^{1}H NMR spectra of ligand HL in DMSO-d_6 solvent. (The peaks observed at 3.33 ppm and 2.45 ppm is due to the residual solvents)

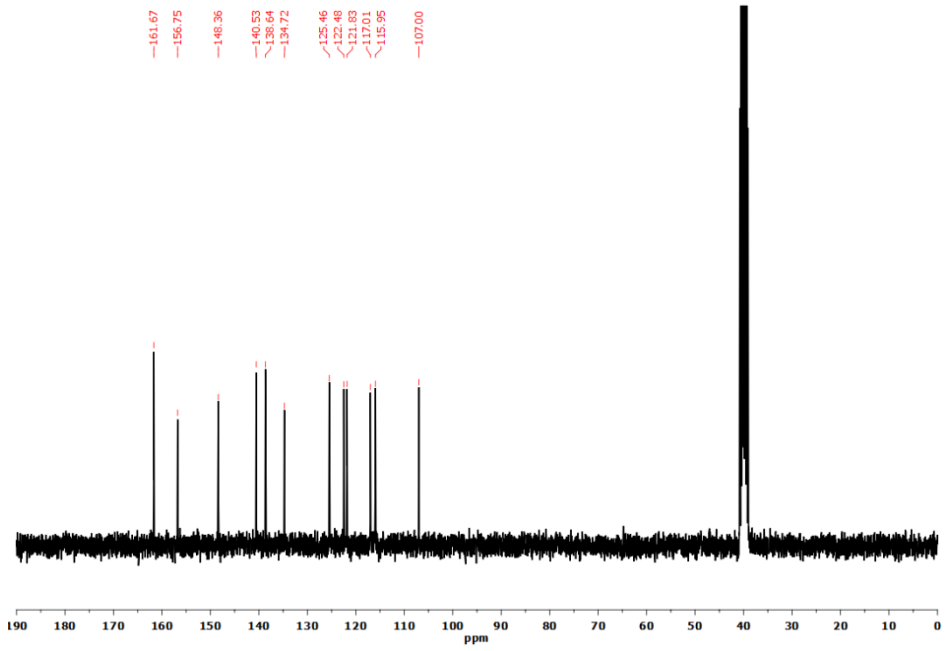

Figure S3. $^{13}C\{^{1}H\}$ NMR spectra of ligand HL in a DMSO-d_6 solvent. (The peak observed at 40 ppm is due to the residual solvent)

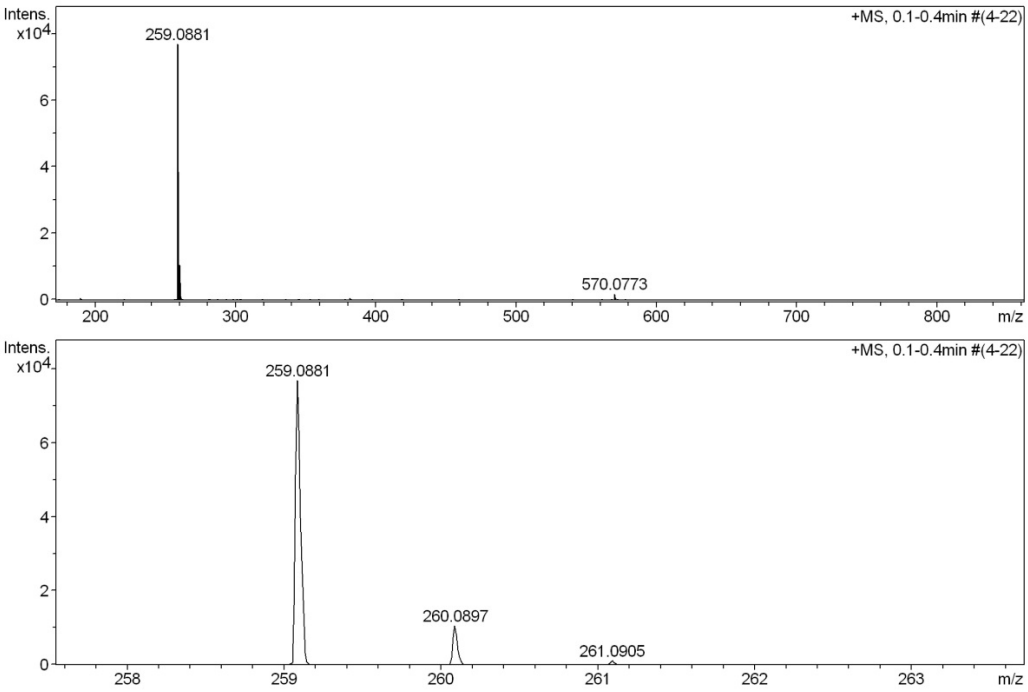

Figure S4. ESI-MS of HL.

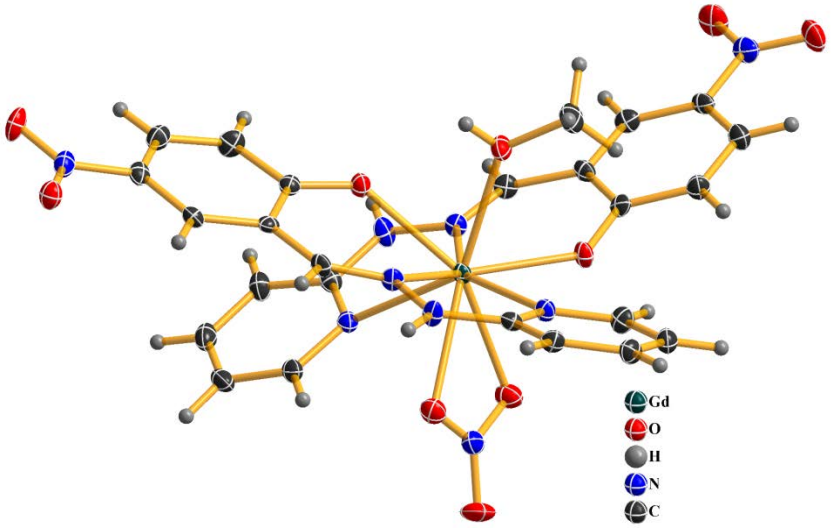

Figure S5. Molecular structure of complex **1**, thermal ellipsoids of 50 % probability level and solvent molecules are omitted for clarity.

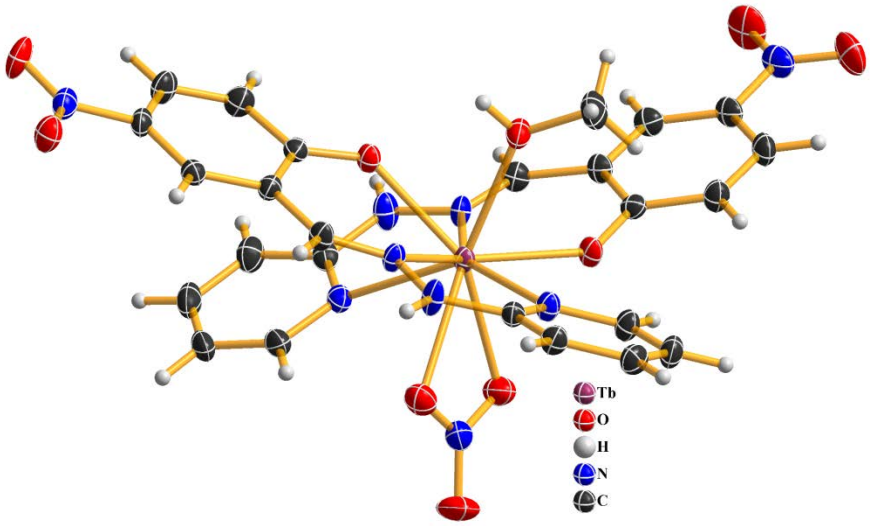

Figure S6. Molecular structure of complex **2**, thermal ellipsoids of 50 % probability level and solvent molecules are omitted for clarity.

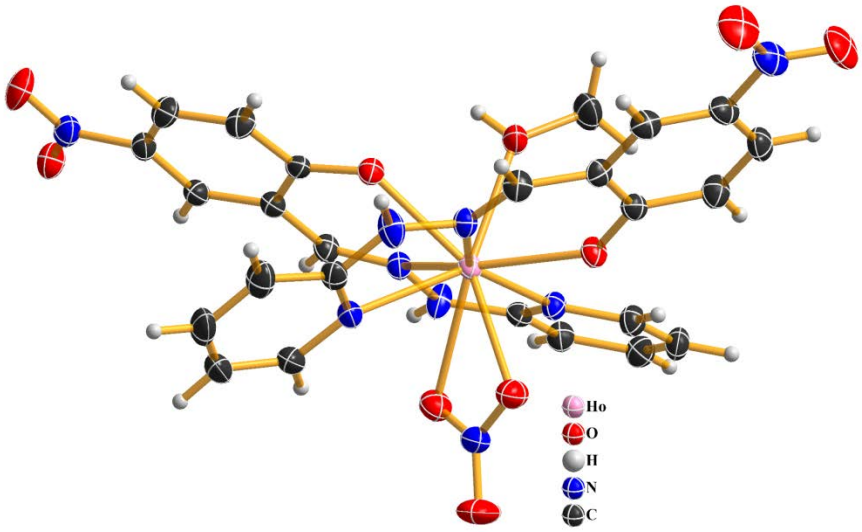

Figure S7. Molecular structure of complex **4**, thermal ellipsoids of 50 % probability level and solvent molecules are omitted for clarity.

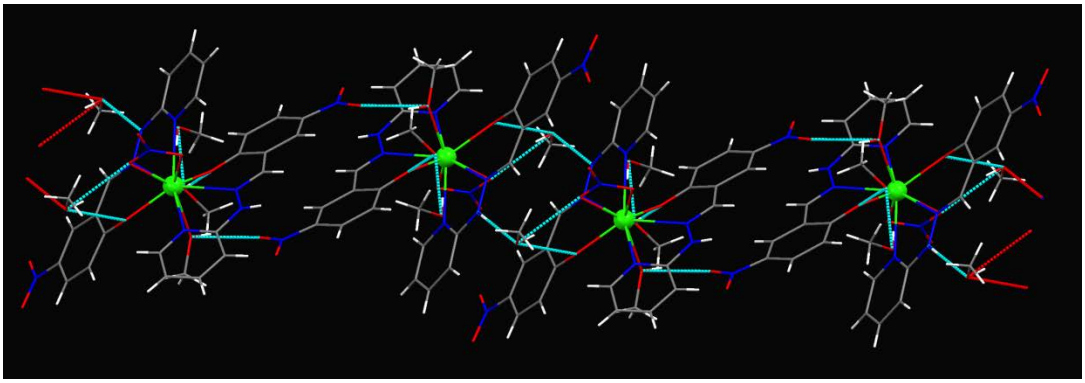

Figure S8. H-bonded one dimensional Zig-Zag chain of complex **3**.

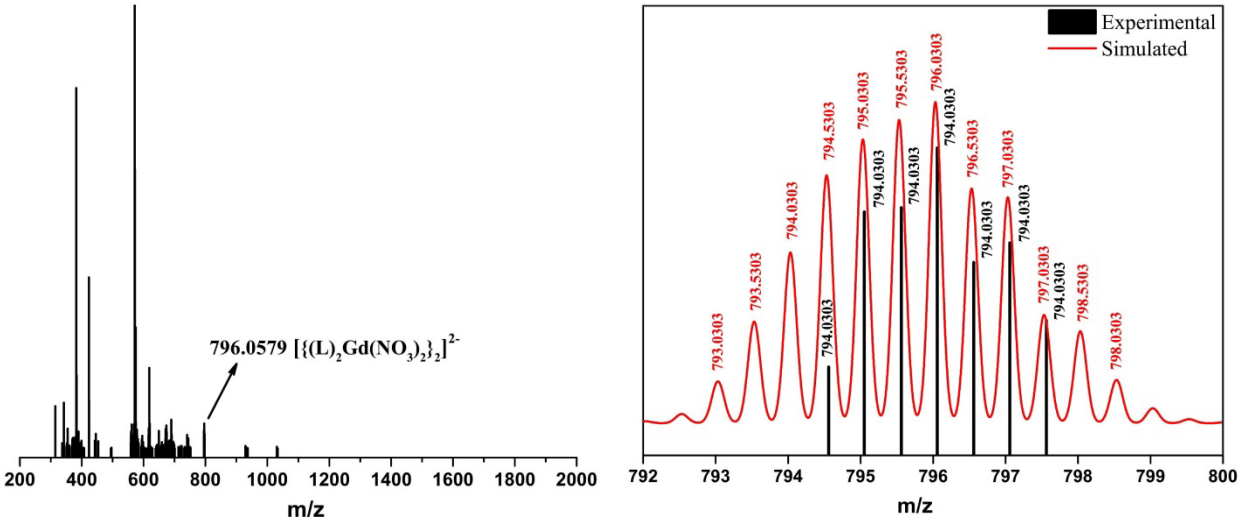

Figure S9. (*Left*) Full range ESI-MS spectrum of complex **1**. (*Right*) Experimental and Simulated pattern of $[\{(L)_2Gd(NO_3)\}_2]^{2-}$.

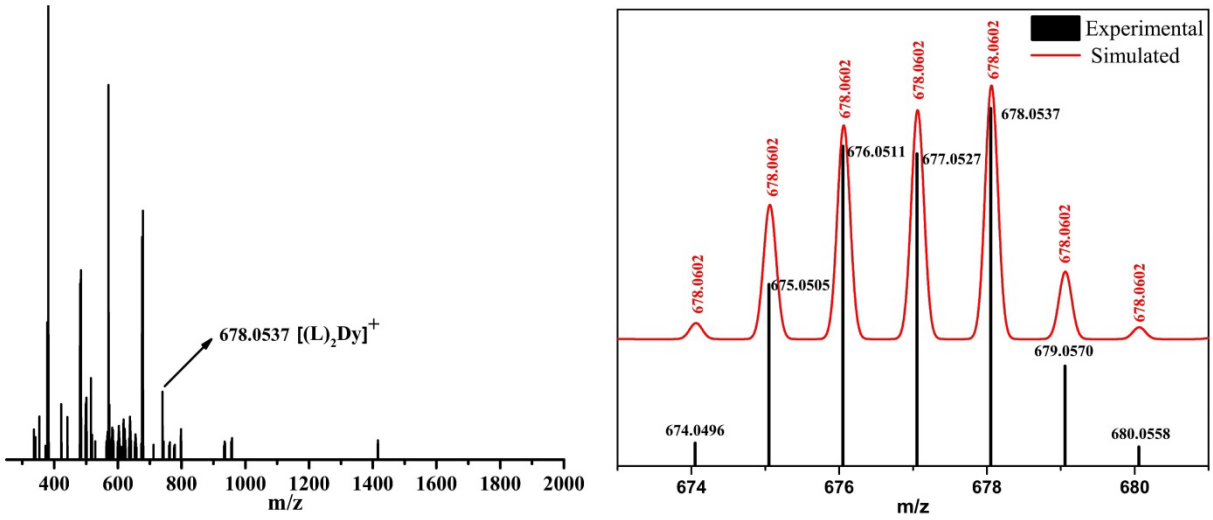

Figure S10. (*Left*) Full range ESI-MS spectrum of complex **3**. (*Right*) Experimental and Simulated pattern of $[(L)_2Dy]^{+}$.

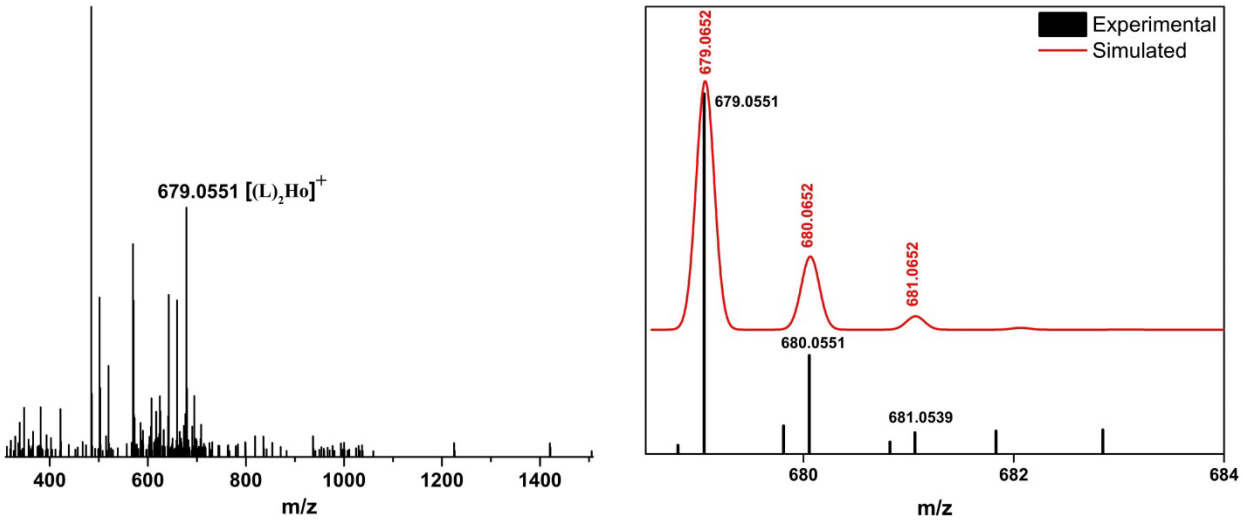

Figure S11. (*Left*) Full range ESI-MS spectrum of complex **4**. (*Right*) Experimental and Simulated pattern of $[(L)_2Ho]^+$.

Table S1. Continuous Shape Measures (CShM) calculations for Ln^{III}

Complex	Structure†												
	EP-9	OPY-8	HBPY-9	JTC-9	JCCU-9	CCU-9	JCSAPR-9	CSAPR-9	JTCTPR-9	**TCTPR-9**	JTDIC-9	HH-9	MFF-9
1_Gd CShM	36.148	20.191	18.225	17.214	9.234	6.930	3.577	1.849	4.111	**1.520**	11.601	10.296	2.147
2_Tb CShM	35.256	20.164	17.958	16.274	9.613	7.989	2.811	2.051	4.027	**1.373**	12.029	10.340	2.135
3_Dy CShM	36.529	20.362	18.298	17.025	9.252	6.966	3.442	1.822	3.960	**1.488**	11.897	10.246	2.198
4_Ho CShM	36.659	20.391	18.384	17.016	9.307	7.072	3.414	1.793	3.894	**1.405**	11.808	10.338	2.154

† *EP-9 = Enneagon (D9h); OPY-9 = Octagonal pyramid (C8v); HBPY-9 = Heptagonal bipyramid (D7h); JTC-9 = Johnson triangular cupola J3 (C3v); JCCU-9= Capped cube J8 (C4v); CCU-9 = Spherical-relaxed capped cube (C4v); JCSAPR-9 = Capped square antiprism J10 (C4v); CSAPR-9 = Spherical capped square antiprism (C4v); JTCTPR-9 = Tricapped trigonal prism J51 (D3h); TCTPR-9 = Spherical tricapped trigonal prism (D3h); JTDIC-9 = Tridiminished icosahedron J63 (C3v); HH-9 = Hula-hoop (C2v); MFF-9 = Muffin (Cs)*

Table S2. Selected bond lengths (Å) and angles (°) of complexes **1**, **2**, and **4.**

–	**Bond lengths** (Å)	**Bond angles** (°)	
		O1–Gd1–O5	117.65(8)
		O1–Gd1–O3	67.90(8)
		O1–Gd1–O4	144.51(9)
		O1–Gd1–N1	70.21(9)
		O2–Gd1–O1	127.46(8)

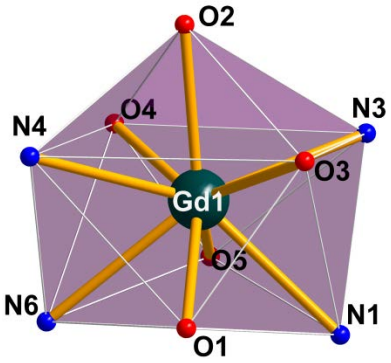 Distorted Spherical tricapped trigonal prism geometry of *Gd1* in complex **1**	Gd1–O1 2.331(2) Gd1–O2 2.285(2) Gd1–O5 2.539(2) Gd1–O3 2.437(2) Gd1–O4 2.472(3) Gd1–N1 2.555(3) Gd1–N3 2.554(3) Gd1–N4 2.553(3) Gd1–N6 2.563(3)	O2–Gd1–O5 114.55(8) O2–Gd1–O3 74.95(9) O2–Gd1–O4 71.32(9) O2–Gd1–N6 124.72(9) O5–Gd1–N1 67.82(9) O5–Gd1–N3 69.79(9) O3–Gd1– O5 42.28(9) O3–Gd1–O4 144.49(9) O3–Gd1–N1 81.43(9) O4–Gd1–O5 50.96(8) O4–Gd1–N1 117.98(9) O4–Gd1–N3 84.87(9) N1–Gd1–N6 95.89(9) N3–Gd1–N1 64.06(9) N3–Gd1–N6 141.44(9) N4–Gd1–N1 145.75(9) N4–Gd1–N3 147.84(9)
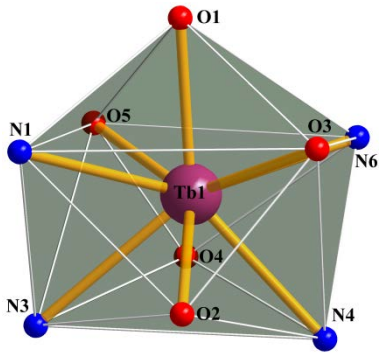 Distorted Spherical tricapped trigonal prism geometry of *Tb1* in complex **2**	Tb1–O3 2.438(2) Tb1–N6 2.541(2) Tb1–O1 2.315(2) Tb1–N1 2.539(2) Tb1–O4 2.552(2) Tb1–O5 2.460(2) Tb1–O2 2.263(2) Tb1–N3 2.541(2) Tb1–N4 2.559(2)	O3–Tb1–N6 94.34(7) O3–Tb1–N1 81.02(7) O3–Tb1–O4 141.61(6) N6–Tb1–O4 124.04(7) N6–Tb1–N3 147.67(6) N6–Tb1–N4 64.32(7) O1–Tb1–O3 68.10(6) O1–Tb1–N6 76.76(6) O1–Tb1–N1 70.17(6) O1–Tb1–N4 68.69(6) N1–Tb1–N6 145.92(6) N1–Tb1–O4 67.79(7) N1–Tb1–N3 64.42(6) N1–Tb1–N4 95.40(7) O4–Tb1–N4 71.93(7) O5–Tb1–N6 85.15(7) O5–Tb1–N1 117.86(7) O5–Tb1–O4 50.86(6) O2–Tb1–O3 74.66(6) O2–Tb1–N6 70.04(6) O2–Tb1–O1 127.18(6) O2–Tb1–N1 138.52(6) N3–Tb1–O4 69.40(7) N3–Tb1–N4 140.85(7)
		O1 Ho1 O4 71.3(4) O1 Ho1 N7 93.9(4) O1 Ho1 N6 77.1(4) O1 Ho1 N3 126.2(4)

<table>
<tr>
<td> 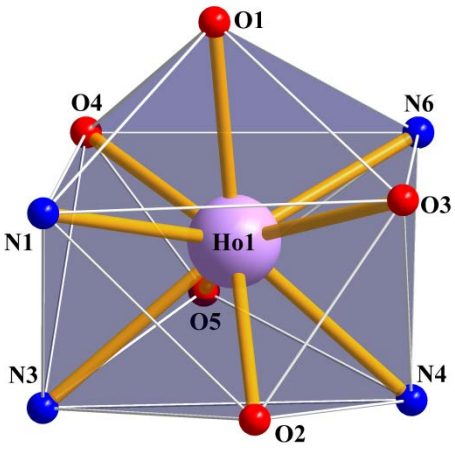

Distorted Spherical tricapped trigonal prism geometry of Ho1 in complex 3</td>
<td>Ho1–O2 2.246(14)
Ho1–O1 2.309(14)
Ho1–O3 2.411(15)
Ho1–O4 2.532(16)
Ho1–O5 2.439(16)
Ho1–N3 2.521(18)
Ho1–N4 2.516(18)
Ho1–N6 2.537(19)
Ho1–N1 2.514(18)</td>
<td>O2–Ho1–O1 126.23(5)
O2–Ho1–O3 74.35(5)
O2–Ho1–O4 114.77(5)
O2–Ho1–O5 71.91(6)
O1–Ho1–O3 67.78(5)
O1–Ho1–O4 118.72(5)
O1–Ho1–O5 144.32(6)
O1–Ho1–N3 127.00(5)
O3–Ho1–O4 141.48(6)
O3–Ho1–O5 144.47(5)
O3–Ho1–N3 77.59(6)
O4–Ho1–N6 71.62(6)
O5–Ho1–O4 51.20(5)
O5–Ho1–N3 84.35(6)
N3–Ho1–O4 69.10(6)
N3–Ho1–N6 140.22(6)
N4–Ho1–O4 124.02(6)
N4–Ho1–N3 147.45(6)
N1–Ho1–N3 65.05(6)
N1–Ho1–N4 145.64(6)</td>
</tr>
</table>

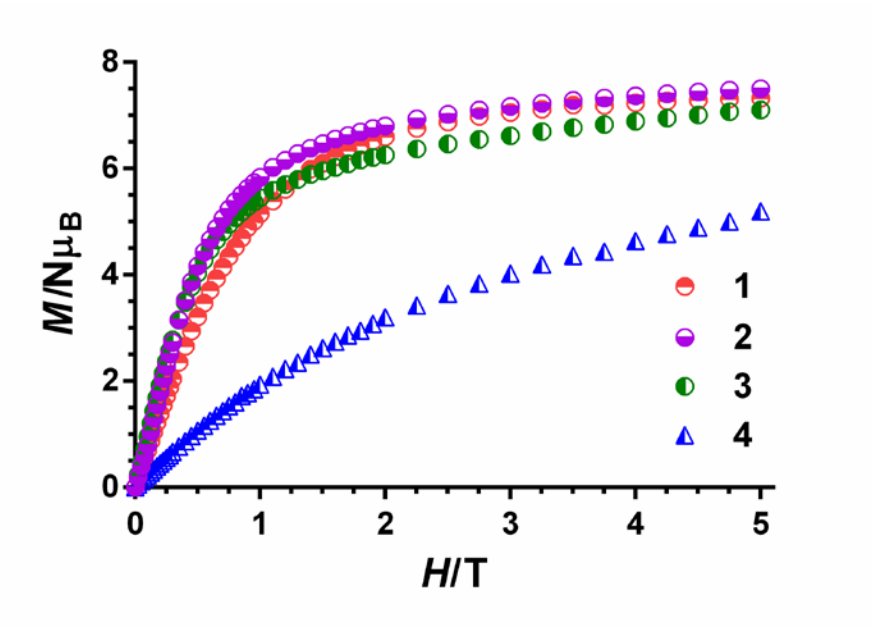

Figure S12. Field dependence of the magnetization at 2 K for complexes **1**-**4**.

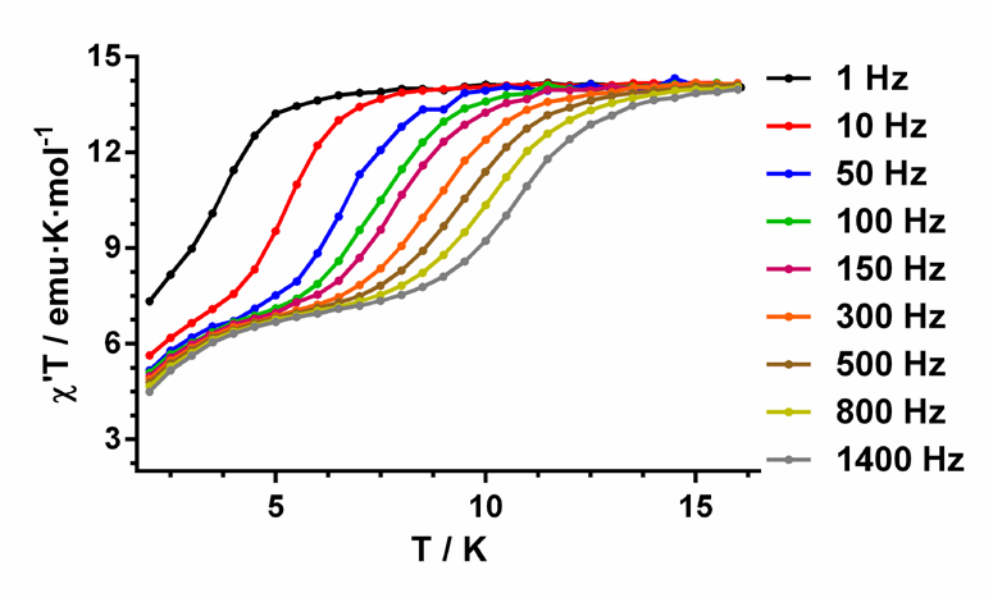

Figure S13. Temperature dependence of $\chi'_M T$ at different frequencies for **3**.

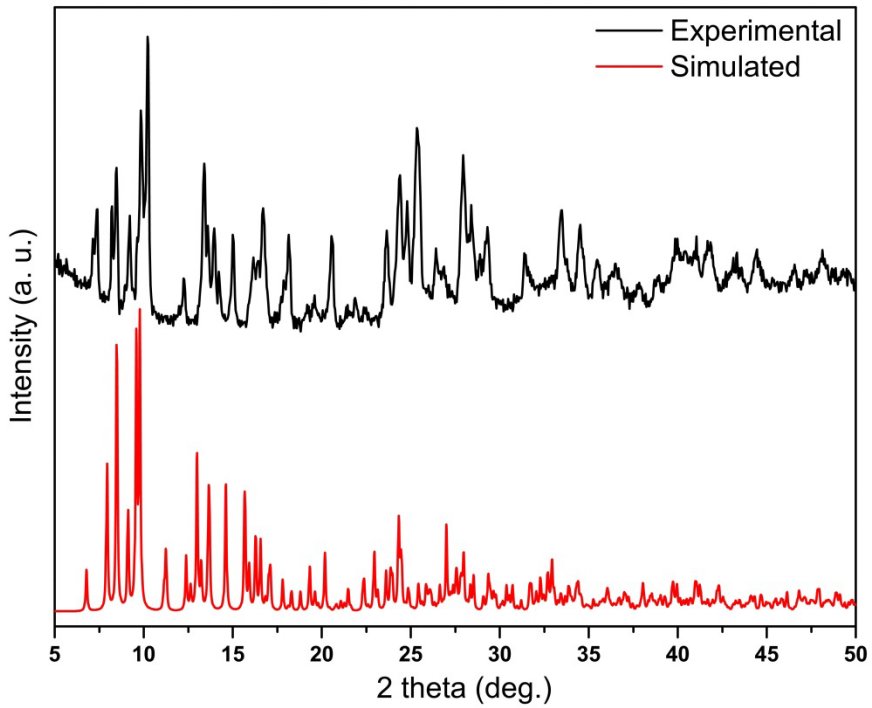

Figure S14. powder XRD pattern of **3'** (The simulated pattern is obtained from SCXRD struture of **3**).

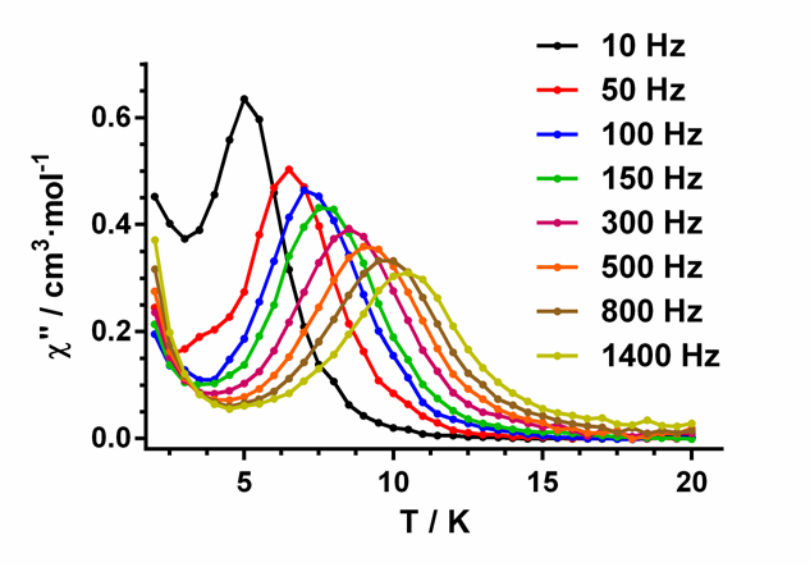

Figure S15. Temperature dependence of χ''_M at different frequencies for **3**.

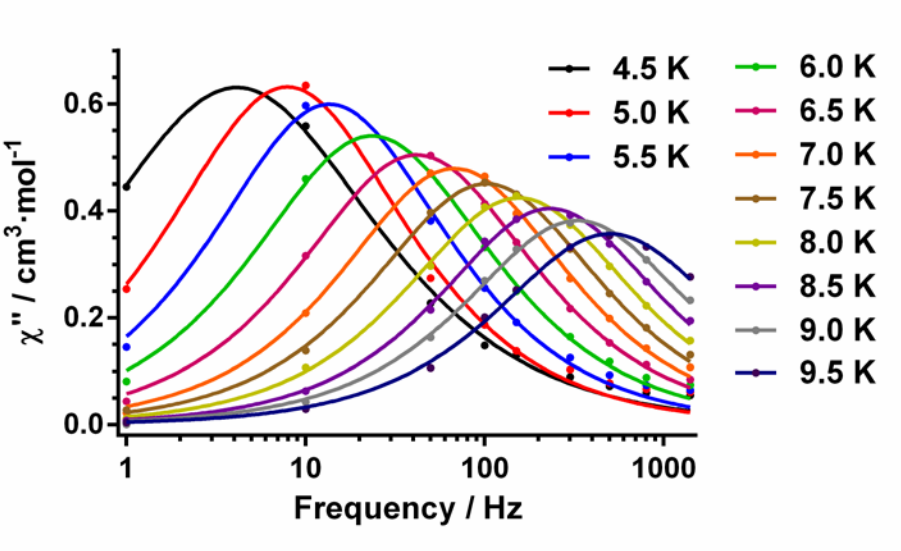

Figure S16. Frequency dependence of χ''_M at different temperatures for **3**.

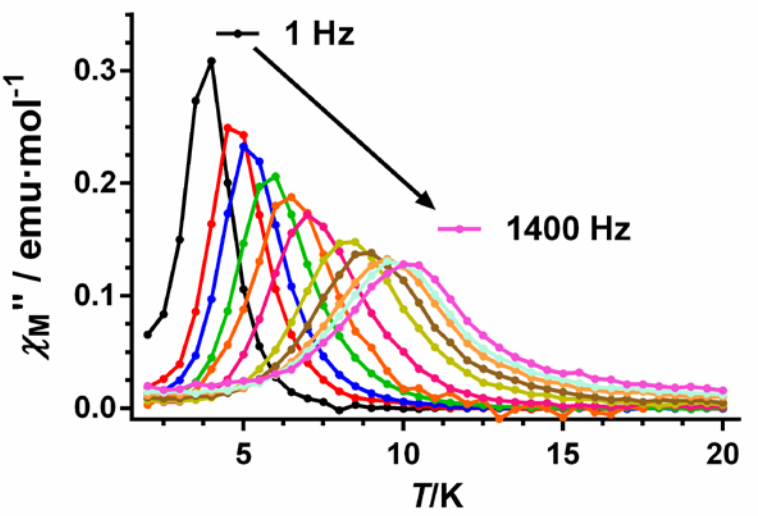

Figure S17. Temperature dependence of χ''_M at different frequencies for **3'**.